Desalination and Water Treatment
www.deswater.com

doi: 10.1080/19443994.2015.1106094

57 (2016) 22764–22773
October

Taylor & Francis
Taylor & Francis Group

Removal of reactive textile dye from aqueous solutions by electrocoagulation in a continuous cell

Abdallah Amour[a], Belkacem Merzouk[b,c,*], Jean-Pierre Leclerc[d], François Lapicque[c]

[a]*Laboratoire de Recherche en Hydraulique Appliquée et Environnement, Faculté de Technologie, Université de Bejaia, Bejaia 06000, Algérie*
[b]*Faculté de Technologie, Département Hydraulique, Université Mohamed Boudiaf de M'sila, B.P. 166, Ichbilia, M'sila 28000, Algérie, Tel. +213 35559494; +213 772782963; Fax: +213 35559494; email: mbelka01@yahoo.fr (B. Merzouk),*
[c]*Laboratoire 3BS, Université de Bejaia, Bejaia 06000, Algérie*
[d]*Laboratoire Réactions et Génie des Procédés (LRGP), UPR3349 CNRS – Université de Lorraine, 1 rue Grandville, B.P. 20451, Nancy, France*

Received 20 March 2015; Accepted 29 September 2015

ABSTRACT

In electrocoagulation (EC), coagulants are delivered *in situ* using the corrosion of sacrificial anodes when a DC voltage is applied. Simultaneously, electrolytic gases (H_2) are generated at the cathode. Aluminum and iron materials are usually used as anodes, the dissolution of which produces hydroxides and polymeric hydroxides. These coagulants are able to destabilize colloidal suspensions and emulsions, to adsorb, neutralize, or precipitate dissolved polluting species, and finally to form flocs that can be removed either by settling or flotation. The purpose of this study was to investigate the effects of the operating parameters, such as initial pH, initial concentration (C_0), residence time (τ), current density (j), and inlet flow rate (Q), on the removal of a red nylosan dye by EC process using aluminum electrode in a continuous electrochemical reactor. FTIR analysis was conducted to interpret the functional groups involved during the EC process. It was found that the increase in the current density up to 100 A m^{-2} had increased the dye removal efficiency and the optimum inlet flow rate for EC process was the minimum at 15 L h^{-1} and it has increased the electrical energy consumption. A rate of abatement of about 90% for turbidity and 97% for color was observed, when the initial concentration of the dye C_0 was lower than 300 mg L^{-1}, current density $j = 300$ A m^{-2}, conductivity $\kappa = 2.54$ mS cm^{-1}, inlet flow rate $Q = 15$ L h^{-1}, residence time $\tau = 35$ min, and initial pH ranged from 2.3 to 8.8. The specific electrical energy consumption was 19.5 kW h per kilogramme of removed dye.

Keywords: Electrocoagulation; Color; Turbidity; Red nylosan dye; Textile wastewater

---

*Corresponding author.

Presented at EuroMed 2015: Desalination for Clean Water and Energy Palermo, Italy, 10–14 May 2015. Organized by the European Desalination Society.

1. Introduction

The textile dyeing and finishing industries generate large quantity of wastewater containing unreacted dyes, suspended solids, dissolved solids, and other auxiliary chemicals. Dye-containing effluent is toxic to the environment since dyes are stable compounds, with low biodegradability and can be carcinogenic [1].

The colored wastewater released into the ecosystem is a dramatic source of esthetic pollution and perturbation in the aquatic life. Conventional methods for dealing with textile wastewater consist of various combinations of biological, physical, and chemical methods [2].

In recent years, investigations have been focused on the treatment of wastewaters using electrocoagulation (EC) owing to the increase in environmental restrictions on effluent wastewater. EC is a simple and efficient method for the treatment of water and wastewaters. It has not been widely accepted because of high initial capital costs as compared to other treatment technologies. EC technique uses a direct current source between metal electrodes immersed in polluted water [3,4]. The electrical current causes the dissolution of metal plates including iron or aluminum into wastewater. The metal ions, at an appropriate pH, can form wide ranges of coagulated species and metal hydroxides that destabilize and aggregate the suspended particles or precipitate and adsorb dissolved contaminants [5].

The most widely used electrode materials in EC process are aluminum and iron. In the case of aluminum, main reactions are as follows:

$$\text{Anode: } Al_{(s)} \rightarrow Al^{3+} + 3e^- \tag{1}$$

$$\text{Cathode: } 3H_2O + 3e^- \rightarrow \frac{3}{2}H_{2(g)} + 3OH^- \tag{2}$$

Al^{3+} and OH^- ions generated by electrode reactions (1) and (2) react to form various monomeric species, which finally transform into $Al(OH)_{3(s)}$ according to complex precipitation kinetics:

$$Al^{3+} + 3H_2O \rightarrow Al(OH)_3 + 3H^+ \tag{3}$$

Freshly formed amorphous $Al(OH)_{3(s)}$ “sweep flocs” have large surface areas, which are beneficial for a rapid adsorption of soluble organic compounds and trapping of colloidal particles. Finally, these flocs are removed easily from aqueous medium by sedimentation or by electroflotation [6–8].

The EC has been considered for a number of wastewaters in a very broad range of nature and composition: in particular oil suspensions [9–12], wastes from textile industry [13–15], tannery [16,17] or food processing [18,19]—a list far from exhaustive.

Examination of the available literature reveals that the treatment mechanism by EC depends on the nature of the waste, as observed in [20,21], and to some extent on the design of EC device and the flow conditions. It also appears that the treatment efficiency has to be considered in terms of various criteria: TOC, COD, turbidity, color, or absorbance at a given wavelength, and concentration of toxic species, e.g. arsenic [12,22] or phosphate [23]. The continuous mode of the EC process has however been less investigated, except in a few studies [8,18,24–27], especially the conditions of floc removal. The results obtained show a good efficiency but with low operational parameters (inlet flow rate $Q \leq 20\ L\ h^{-1}$).

In this regard, the objective of the paper is thus to study the operation of this new design of EC reactor by examining the effects of the operating parameters, such as the current density (j), residence time (τ), initial concentration (C_0), and initial pH and inlet flow rate (Q), on color removal efficiency of a synthetic wastewater containing red nylosan dye.

2. Materials and methods

2.1. Synthetic wastewater

Red nylosan dye N-2RBL (sodium 6-amino-5-[[4-chloro-3-[[(2,4-dimethylphenyl) amino] sulfonyl] phenyl]azo]-4-hydroxynaphthalene-2-sulfonate) was used for preparing synthetic dye wastewater. Its chemical

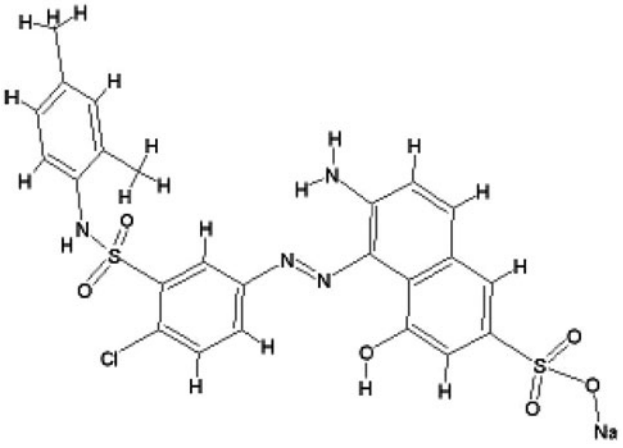

Fig. 1. The chemical structure of red nylosan dye.

Table 1
Main characteristics of red nylosan dye

Color index number	Acid red 336
CAS registry number	71873-39-7
Molecular formula	$C_{24}H_{21}$ ClN_4O_6 S_2, Na
Molecular weight	587.97 g mol^{-1}
UV absorption	λ_{max} 502 nm

structure is shown in Fig. 1. Principal characteristics of this compound are given in Table 1.

The synthetic wastewater was prepared by dissolving the dye into deionized water and was diluted according to the desired concentration (50–300 mg L^{-1}). The pH was adjusted to 7.5 ± 0.3 with NaOH and the conductivity was adjusted to 2,500 ± 25 μS cm^{-1} with NaCl. The values of pH and conductivity were chosen to simulate the properties of wastewater from a textile industry. The initial concentration of 50 mg L^{-1} was selected because it provided a noticeable color and a chemical oxygen demand (COD) value in the same order of magnitude as the effluent from the textile factory [7,13,28]. The typical characteristics of the synthetic textile wastewater to be treated are presented in Table 2.

2.2. Experimental setup

A single reactor for both metal dissolution and solid settling has been designed and constructed as the continuous treatment EC reactor of industrial wastewaters: the long cell consisted of two chambers with a series of most different volumes and flow conditions. The continuous flow pilot-scale EC reactor is shown in Fig. 2. The waste liquid is pumped into the electrochemical chamber provided with two aluminum (purity of Al was 98%) plate anodes and cathodes (dimension 240 × 20 × 10 mm) used as vertical Al electrodes. The electrodes were 100% dipped into an aqueous solution in a Perspex reactor. The gaps between the two neighboring electrode plates were kept constant at 10 mm for all the experiments. The electrodes were connected in bipolar mode to a laboratory DC power supply ($GPS3303_{3CH}$) providing current in the range of 00–10 A, that was held constant for a given experimental run.

Table 2
Physicochemical characteristics of the synthetic textile wastewater investigated

Parameter	Synthetic wastewater
pH_0	7.74
Turbidity (NTU)	85
COD (mg O_2 L^{-1})	123
Conductivity (μS cm^{-1})	2,500
Temperature (°C)	20
Suspended solids SS (mg L^{-1})	105
Color	Dark red

The reactor is configured with an electrochemical chamber of nearly 3.1 L volume and a large sedimentation and flotation tank of 5.5 L volume.

The two compartments were connected by a triangular groove and the wastewater passed from the first chamber to the second one by overflow. The volume V_2 = 5.5 L of the tank and the position of outlet tube were designed to avoid the presence of solid particles in the effluent stream. The sludge was essentially recovered by flotation. The floating materials were removed continuously from the second compartment by overflow, whereas the few more dense materials could settle. The solution to be treated was continuously circulated in the flow circuit by means of a peristaltic pump "'Heidolph PD 5006, Pump drive"' providing flow in the range of 0–60 L h^{-1}. The influence of various parameters on the dye-removing process was achieved using synthetic wastewater in a continuous EC reactor.

2.3. Analytical methods

Samples (40 mL) were collected in the reservoir every 05 min until the steady-state regime was achieved. In practice, the reactor reaches the steady-state conditions approximately at mean residence time. This is because the reaction at the electrodes is very fast and the reactor behaves as a plug flow reactor in the electrochemical cell.

Dye concentration was estimated from its absorbance characteristics in the UV–vis range (250–800 nm), using the wavelength that provided the maximum intensity (λ_{max} = 502 nm) and a UV–vis spectrophotometer (Shimadzu-1240 S). Solution conductivity and pH were measured using a Hanna EC214 conductimeter and a Hanna pH210 pH meter, respectively. The colorimetric micro-method (HACH (Loveland, Colorado) method 8000) with an excess of hexavalent chromium and subsequent measurement of the optical density using a HACH 2400 spectrophotometer (Loveland, Colorado) was used for the soluble COD determination. For COD measurements, the calibration curves were obtained using potassium hydrogen phtalate (Fluka, analytical grade). The UV–vis spectra of the filtered samples were measured

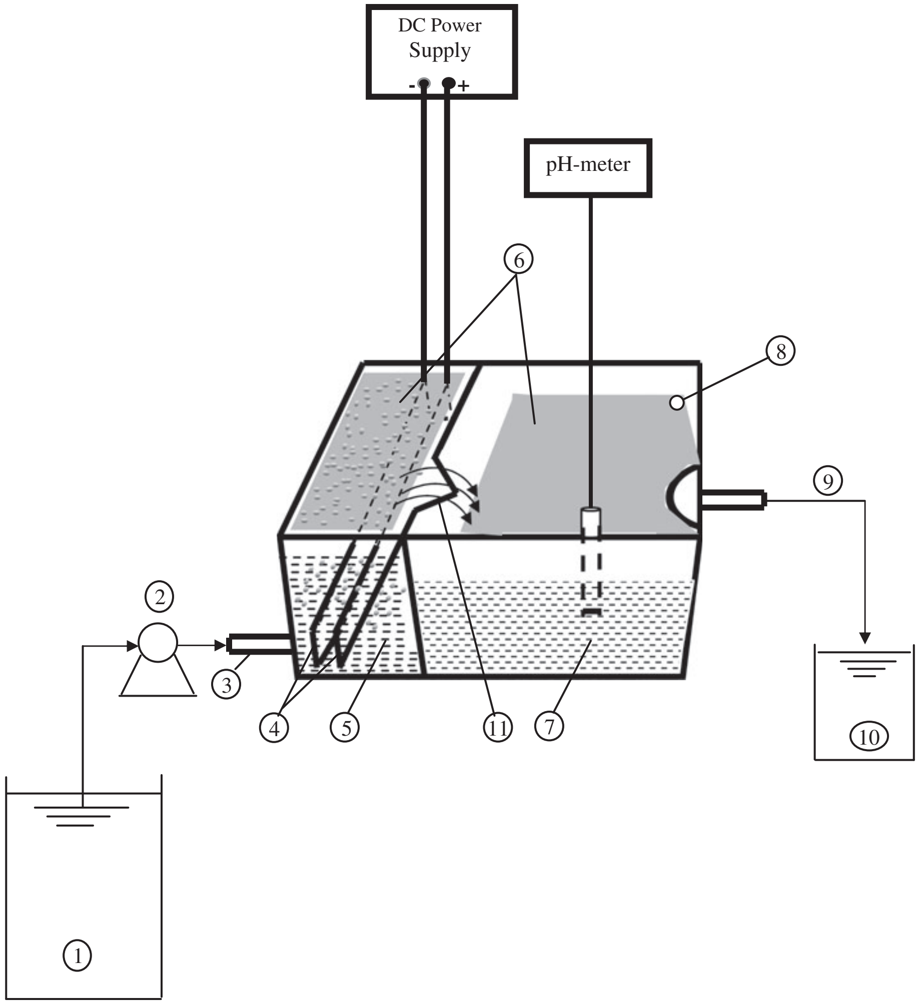

Fig. 2. Experimental setup of continuous EC cell.
Notes: (1) wastewater tank, (2) peristaltic pump, (3) inlet of the first compartment, (4) electrodes, (5) first chamber, (6) sludge, (7) second chamber, (8) sludge exit (overflow), (9) treated effluent outlet, (10) treated water tank, and (11) outfall.

with an Anthelie Light (Secomam, Domont, France) spectrophotometer; light absorbance was measured between 200 and 600 nm using 1-cm path quartz cells. Turbidity of the waters was measured using a Hanna HI88703 spectrophotometer. Data were given in Nephelometric Turbidity Unit (NTU).

Color in terms of absorbance and turbidity removal efficiencies (Y_{Col}, Y_{Tr}) was expressed as a percentage and defined as follows:

$$Y\,(\%) = \frac{C_0 - C_f}{C_0} \times 100 \tag{4}$$

The subscripts, "0" and "f", are used to distinguish concentration in the inlet and the outlet streams of the EC cell.

The specific electrical energy consumption (SEEC) per kg dye removed (SEEC) and the specific electrode consumption per kg dye (μ_{Al}) were calculated from the liquid absorbance as follows:

$$\mathrm{SEEC}\left(\frac{\mathrm{kW\ h}}{\mathrm{kg\ dye}}\right) = \frac{\mathrm{UI}}{1{,}000\,Q\,(C_0\,Y_{\mathrm{COL}})} \tag{5}$$

$$\mu_{\mathrm{Al}}\left(\frac{\mathrm{kg\ Al}}{\mathrm{kg\ dye}}\right) = \frac{3{,}600\,M_{\mathrm{Al}}\,I\,\phi_{\mathrm{Al}}}{3F}\,\frac{1}{Q\,(C_0\,Y_{\mathrm{COL}})} \tag{6}$$

using initial dye concentration C_0 (kg m^{-3}), current intensity I (A), cell voltage U (V), residence time τ (h), liquid volume V (m^3), molar weight of aluminum $M_{\mathrm{Al}} = 0.027$ kg mol^{-1}, Faraday's constant F (96,487 C mol^{-1}), and the faradic yield ϕ_{Al} of Al dissolution.

ϕ_{Al} was estimated as the ratio of the weight loss of the aluminum electrodes during the experiments Δm_{exp} and the amount of aluminum consumed theoretically at the anode Δm_{th}:

$$\phi_{\mathrm{Al}} = \frac{\Delta m_{\mathrm{exp}}}{\Delta m_{\mathrm{th}}} = \frac{3F}{3,600\ M_{\mathrm{Al}} I \tau}\,\Delta m_{\mathrm{exp}} \tag{7}$$

This parameter depends upon the pH and the amount of other species present in solution, for example coexisting anions [29].

3. Results and discussion

3.1. Effect of current density on the color and turbidity removal

Since the decolorization is the main objective of the treatment of textile wastewaters, absorbance variation is the first parameter to follow up. In all electrochemical processes, current density is the most important parameter for controlling the reaction rate within the electrochemical reactor [30]. It is well known that current density determines the production rate of coagulant, adjusts also bubble production, and hence affects the growth of flocs [3,5]. To investigate the effect of current density j on the efficiency of color and turbidity removal, continuous EC process was carried out using various current densities at fixed inlet concentration $C_0 = 50$ mg L^{-1} with influent pH 7.74 and an inlet flow rate $Q = 25.2$ L h^{-1}. The data monitored for 60-min operation are presented in Fig. 3(a) and (b).

The absorbance decreases down from 0.38 to 0.01 and turbidity from 85 to 1.43 NTU. As clearly seen from Fig. 4(a), the calculated specific energy consumption per kg dye removed (SEEC) increased with increasing applied current densities as expected.

Energy consumption varies with the square of the current density and generates heat by Joule effect; the SEEC values increased accordingly from 3.2 to 31.3 kW h kg^{-1} dye removed for 45-min operation time.

An increase in current density from 100 to 400 A m^{-2} yielded an increase in the efficiency of color removal from 85.5 to 99.3%. This could be expected: when the current density increases, the amount of $\mathrm{Al^{3+}}$ cations released by the anode and therefore of $\mathrm{Al(OH)_3}$ particles also increases. However, the difference between the curves corresponding to different current densities became small when j was higher than 200 A m^{-2}. An optimum current density can therefore be defined. Indeed, when the increase in Y_{Col} with j is slight, the disadvantages of working at high current densities prevail: first, the amount of sludge increases typically as j; then, the same stands for electrode material consumption, while energy consumption rises as j^2. These trends were confirmed experimentally in Fig. 4(a) and (b) for SEEC and μ_{Al}, respectively, and they agree qualitatively with data already reported in the literature for textile dye wastewaters [3,7,31–36]. The SEEC was 19.5 kW h per kilogramme of removed dye for $j = 300$ A m^{-2} which corresponds to 96.6% of removal turbidity.

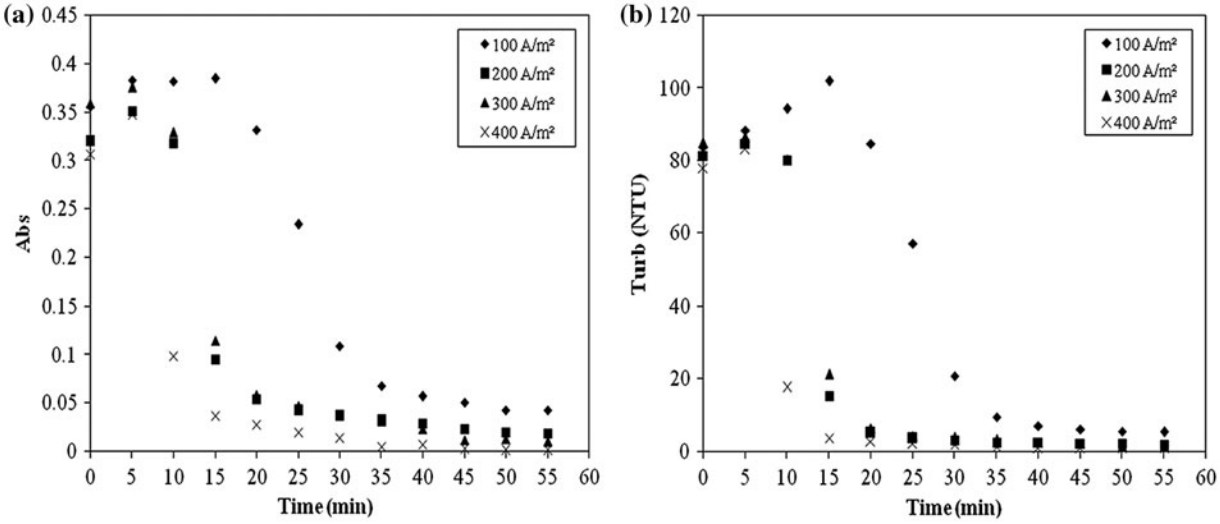

Fig. 3. Evolution of absorbance (a) and turbidity (b) during the treatment for different current densities j: $C_0 = 50$ mg L^{-1}, initial pH 7.74, $Q = 15$ L h^{-1}, $e = 1$ cm, $\kappa = 2.5$ mS cm^{-1}.

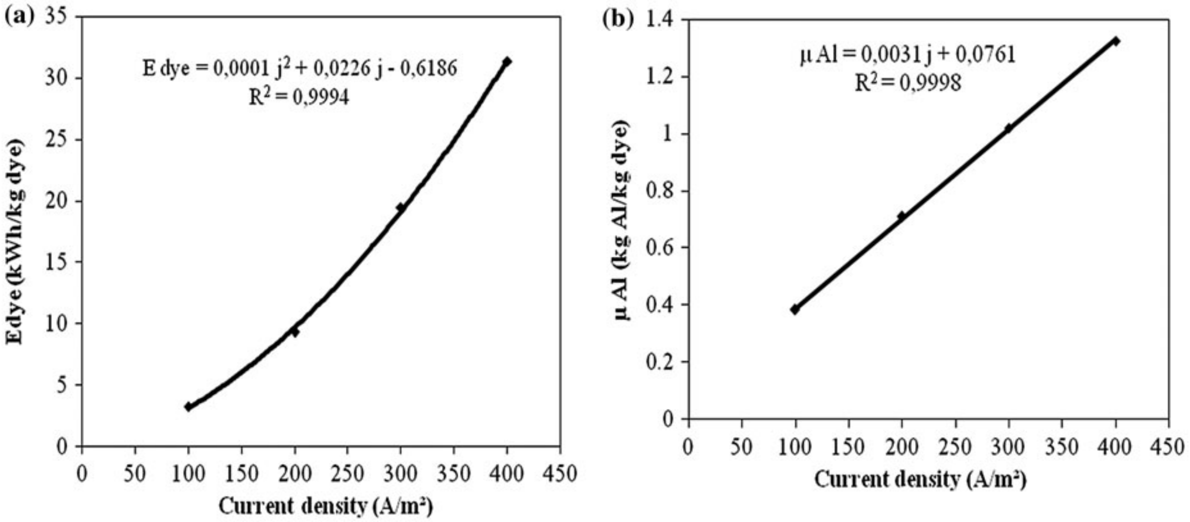

Fig. 4. Effect of current density j on energy consumption (SEEC) (a) and electrode consumption (μ_{Al}) (b) $C_0 = 50$ mg L^{-1}, initial pH 7.74, $Q = 15$ L h^{-1}, $e = 1$ cm, $\kappa = 2.5$ mS cm^{-1}.

3.2. Effect of inlet flow rate on the absorbance and color removal

In order to investigate the effect of the residence time on the absorbance and color removal efficiency, the inlet flow rate Q was progressively increased from 15 to 60 L h^{-1}, respectively, for $j = 300$ A m^{-2} and influent pH 7.58.

As shown in Fig. 5(a) and (b), the continuous EC process functions for all studied inlet flow rates and the color removal ratio reach 90%.

These figures show that Y_{Col} presents a maximum at a flow of approximately 15 L h^{-1}, with a value of 97.2% after 55 min of treatment and 91.4% with 35 min of treatment which is the residence time.

On the other hand for $Q = 38.7$ L h^{-1}, $Y_{Col(max)}$ is 93% with 35 min of treatment against 92.2% with 55 min of treatment. For $Q = 60$ L h^{-1}, $Y_{Col(max)}$ is 90.2% after 55 min of treatment. The optimal rate of feed could thus be taken between 15 and 38.7 L h^{-1}. Comparing the results obtained in this study with similar ones [8,18,24–27,37], the inlet flow rates do not

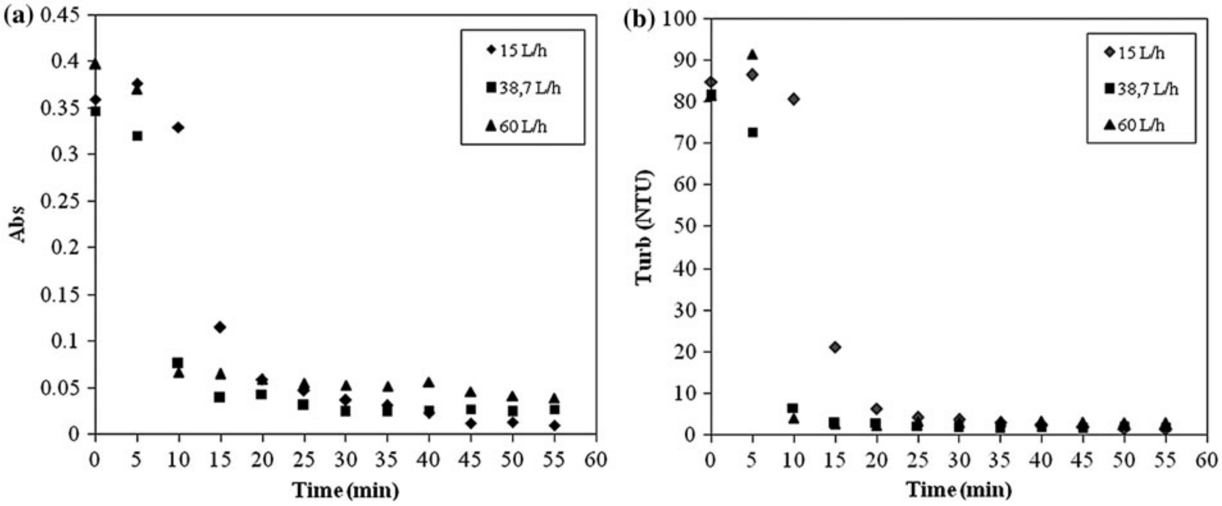

Fig. 5. Evolution of absorbance (a) and turbidity (b) during the treatment for different inlet flow rates Q: $C_0 = 50$ mg L^{-1}, initial pH 7.58, $j = 300$ A m^{-2}, $e = 1$ cm, $\kappa = 2.54$ mS cm^{-1}.

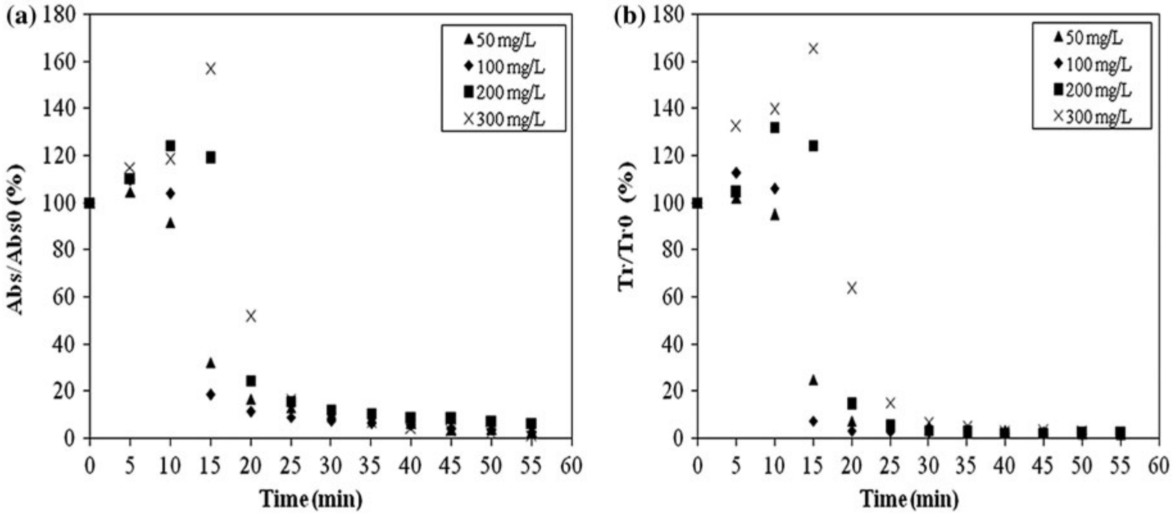

Fig. 6. Evolution of absorbance (a) and turbidity (b) during the treatment for different initial concentration C_0: $Q = 15$ L h^{-1}, initial pH 7.74, $j = 300$ A m^{-2}, $e = 1$ cm, $\kappa = 2.5$ mS cm^{-1}.

exceed 20 L h^{-1} to obtain a color removal ratio higher than 80%.

3.3. *Effect of initial concentration on the absorbance and color removal*

Fig. 6(a) and (b) illustrates the evolution of removal efficiency of color and turbidity removal as a function of the influent dye concentration, using the optimum conditions obtained previously for current, residence time, and pH. In this figure, dye solutions with different concentrations in the range of 50–300 mg L^{-1} were treated by continuous EC process. The data show that the continuous EC process gave satisfactory results for all the concentrations studied, as Y_{Col} was always higher than 97.2% and Y_{Tr} higher than 97.4%.

3.4. *Effect of initial pH on the absorbance and color removal*

It has already been established that pH is a key operating factor influencing the performance of EC process [7,13,14,30,36–39]. To examine its effect, the

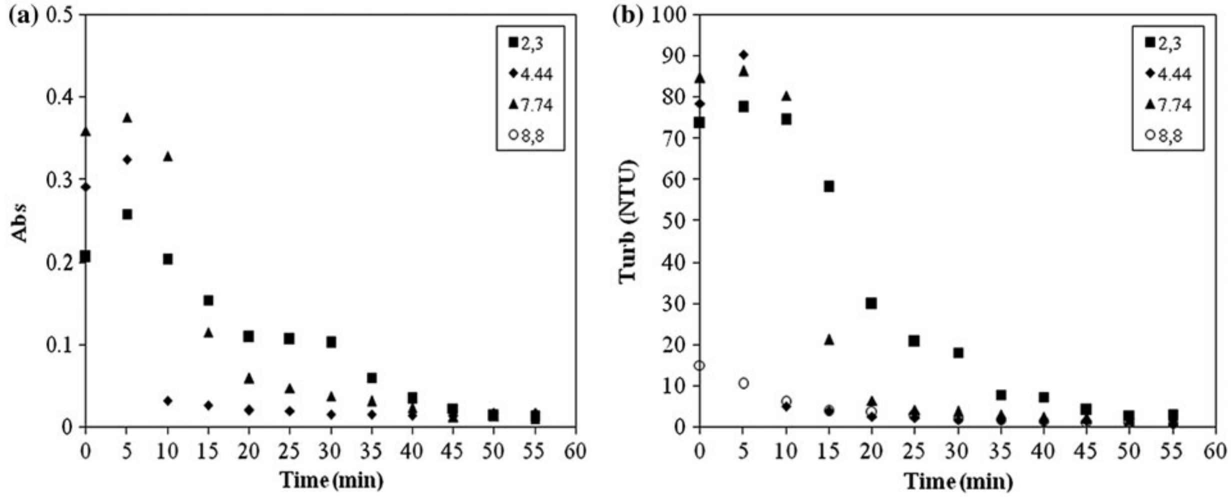

Fig. 7. Evolution of absorbance (a) and turbidity (b) during the treatment for different values of initial pH: $C_0 = 50$ mg L^{-1}, $j = 300$ A m^{-2}, $Q = 15$ L h^{-1}, $e = 1$ cm, $\kappa = 2.5$ mS cm^{-1}.

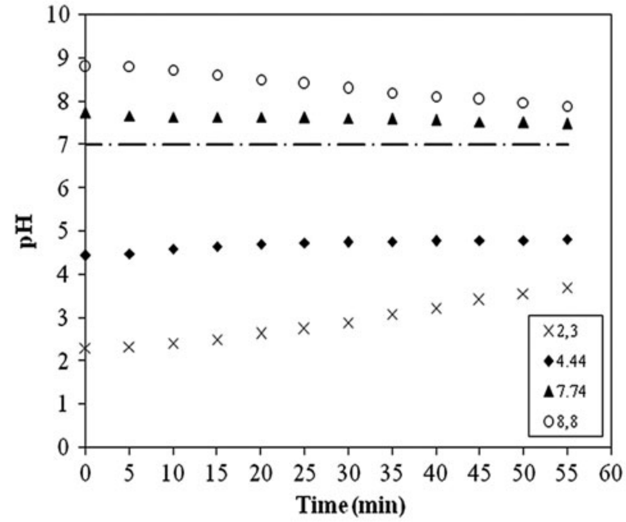

Fig. 8. Evolution of pH values during EC for different values of initial pH: $C_0 = 50$ mg L^{-1}, $j = 300$ A m^{-2}, $Q = 15$ L h^{-1}, $e = 1$ cm, $\kappa = 2.5$ mS cm^{-1}.

pH of the wastewater was adjusted to the desired value for each experiment by adding either sodium hydroxide or sulfuric acid.

Fig. 7(a) and (b) shows that Y_{Col} and Y_{Tr} exceed 93% for all the pH studied. The maximum efficiency of color removal was observed at pH 7.74 with $Y_{Col} = 97.2\%$ and $Y_{Tr} = 98.3\%$.

It is desirable that final pH values are near neutrality after EC process. Fig. 8 demonstrates pH fluctuation during EC. This was observed by several authors [7,18,33,36,37]. Its evolution depends on initial pH: whatever the initial pH values, acidic or basic, there is an EC buffering trend toward pH around 7. This is explained by a balance between OH^- production and consumption, preventing high changes in pH [5,36,37], which is advantageous for wastewater treatments.

3.5. Fourier transform infrared spectroscopy study

Fourier transform infrared spectroscopy (FTIR) analysis helps in understanding the reaction mechanism as it identifies the functional groups involved during the EC process. The spectra were recorded in region of 4,000–400 cm^{-1} with a resolution of 2 cm^{-1} in an IR spectrophotometer (Perkin-Elmer, RZX) (Fig. 9). The FTIR spectrum of the dye before treatment by EC (RN 1) shows a peak at 3,402.2 cm^{-1} due to the presence of O–H and N–H stretching vibrations, while a peak at 2,923.9 cm^{-1} is due to C–H group of alkyl chain. The peaks at 1,624 cm^{-1} are due to the

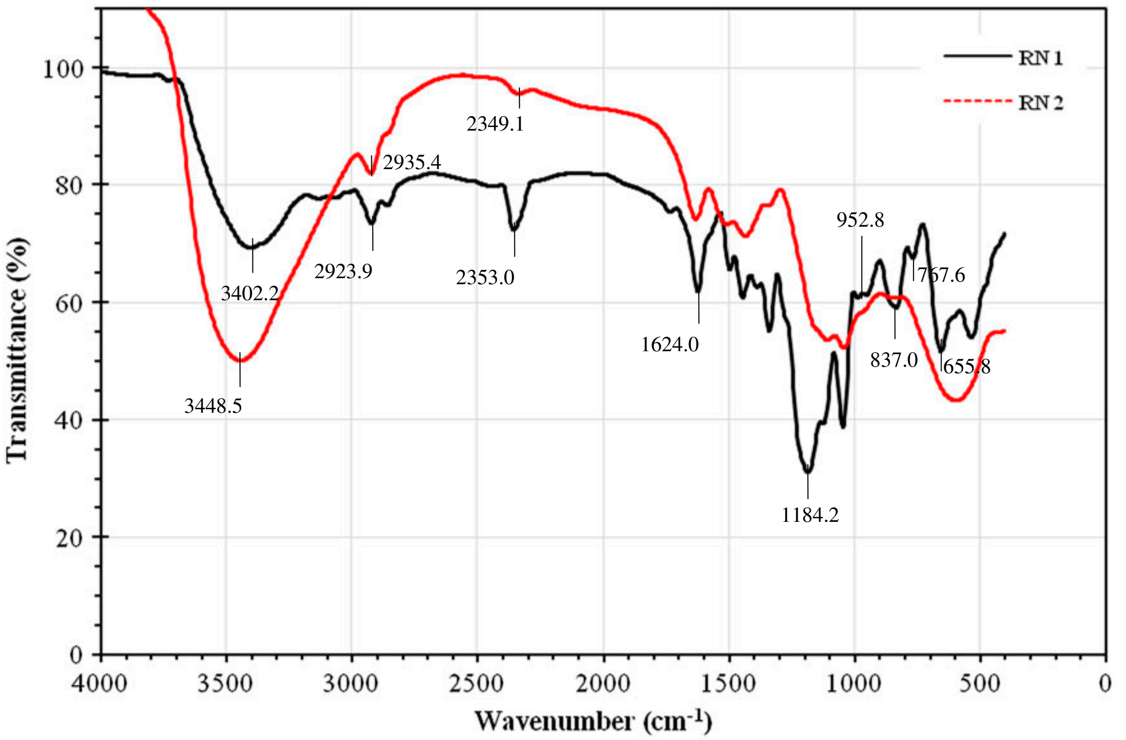

Fig. 9. FTIR spectrum of Acid Red 336 before and after the EC process.

presence of carbonyl groups. The peak at 1,184.2 cm^{-1} shows the presence of C–N (s) vibration. The bands at 952.8 and 837 cm^{-1} are a characteristic of C–Cl (s) vibrations. The peaks at 767.6 and 655.8 cm^{-1} are due to the presence of N–H vibrations due to secondary amines. Comparing the FTIR spectra of the dye before and after EC process (RN 1 and RN 2), there was a marked shift in the band from 2,349.7 to 3,448.5 cm^{-1}.

4. Conclusions

A series of experiments was performed in order to find the effects of operating parameters for decolorization of textile dye wastewater EC of a continuous mode. Dye removal by continuous EC process was affected by current density, initial pH, and inlet flow rate.

Our results suggest an opportunity for the application of continuous EC process to remove color and turbidity from wastewater. An increase in the current density increases the kinetics rate due to the faster dissolution of aluminum. Consequently, the reaction time is faster for a given removal efficiency which allows to increase the productivity of the continuous reactor by working at higher flow rate. The results showed that about 90% for turbidity and 97% for the color were observed, when the initial concentration of the dye C_0 was lower than 300 mg L^{-1}, current density $j = 300$ A m^{-2}, conductivity $\kappa = 2.54$ mS cm^{-1}, inlet flow rate $Q = 15$ L h^{-1}, residence time $\tau = 35$ min, and initial pH ranged from 2.3 to 8.8. The SEEC was 19.5 kW h per kilogramme of removed dye. The EC continuous mode was determined to be an efficient and viable process for achieving a high degree of dye removal from textile wastewater.

Nomenclature

C_0 — dye concentration (kg m^{-3})
C_{Al} — concentration of dissolved aluminum (kg m^{-3})
COD — chemical oxygen demand (mg O_2 L^{-1})
EC — electrocoagulation
F — Faraday's constant (96,487 C mol^{-1})
FTIR — Fourier transform infrared spectroscopy
I — current (A)
j — current density (A m^{-2})
M_{Al} — molar mass of aluminum (0.0267 kg mol^{-1})
Q — inlet flow rate (L h^{-1})
RN — red nylosan
S — electrode surface area (m^2)
SEEC — specific electrical energy consumption (kW h kg^{-1} dye removed)
SS — suspended solids (mg L^{-1})
t — time (h)
U — measured potential (V)
V — reactor volume (m^3)
Y_{Col} — color removal efficiency (%)
Y_{Tr} — turbidity removal efficiency (%)

Greek

Δm_{exp} — experimental weight loss of Al electrode (kg)
Δm_{th} — theoretical weight loss of Al electrode (kg)
κ — wastewater conductivity (μS cm^{-1})
λ_{max} — maximum wavelength of the absorption spectrum (nm)
μ_{Al} — specific consumption of the anode (kg Al kg^{-1} dye removed)
τ — liquid residence time in the reactor (s)
ϕ_{Al} — faradic yield of Al dissolution

References

[1] P. Gregory, Azo dyes: Structure-carcinogenicity relationships, Dyes Pigm. 7(1) (1986) 45–56.

[2] N. Daneshvar, D. Salari, A. Niaei, M.H. Rasoulifard, A.R. Khataee, Immobilization of TiO_2 nano-powder on glass beads for the photocatalytic decolorization of an azo dye C.I. Direct Red 23, J. Environ. Sci. Health 40 (2005) 1–13.

[3] B. Merzouk, K. Madani, A. Sekki, Using electrocoagulation–electroflotation technology to treat synthetic solution and textile wastewater, two case studies, Desalination 250 (2010) 573–577.

[4] E.-S.Z. El-Ashtoukhy, N.K. Amin, Removal of acid green dye 50 from wastewater by anodic oxidation and electrocoagulation—A comparative study, J. Hazard. Mater. 179 (2010) 113–119.

[5] G. Chen, Electrochemical technologies in wastewater treatment, Sep. Purif. Technol. 38 (2004) 11–41.

[6] M. Kobya, O.T. Can, M. Bayramoglu, M. Sozbir, Operating cost analysis of electrocoagulation of textile dye wastewater, Sep. Purif. Technol. 37 (2004) 117–125.

[7] B. Merzouk, B. Gourich, A. Sekki, K. Madani, M. Chibane, Removal turbidity and separation of heavy metals using electrocoagulation–electroflotation technique, J. Hazard. Mater. 164 (2009) 215–222.

[8] M.Y.A. Mollah, S.R. Pathak, P.K. Patil, M. Vayuvegula, T.S. Agrawal, J.A.G. Gomes, M. Kesmez, D.L. Cocke, Treatment of orange II azo-dye by electrocoagulation (EC) technique in a continuous flow cell using sacrificial iron electrodes, J. Hazard. Mater. 109 (2004) 165–171.

[9] J.P.F. Koren, U. Syversen, State of the-art: Electroflocculation, Filtr. Sep. 32 (1995) 146–156.

[10] L. Sanchez-Calvo, J.P. Leclerc, G. Tanguy, M.C. Cames, G. Paternotte, G. Valentin, A. Rostan, F. Lapicque, An electrocoagulation unit for the purification of soluble oil wastes of high COD, Environ. Progress 22 (2003) 57–65.

[11] M. Khemis, G. Tanguy, J.P. Leclerc, G. Valentin, F. Lapicque, Electrocoagulation for the treatment of oil suspensions, Process Saf. Environ. Prot. 83(1) (2005) 50–57.

[12] P. Ratna Kumar, S. Chaudhari, K.C. Khilar, S.P. Mahajan, Removal of arsenic from water by electrocoagulation, Chemosphere 55 (2004) 1245–1252.

[13] I. Zongo, A.H. Maiga, J. Wéthé, G. Valentin, J.-P. Leclerc, G. Paternotte, F. Lapicque, Electrocoagulation for the treatment of textile wastewaters with Al or Fe electrodes: Compared variations of COD levels, turbidity and absorbance, J. Hazard. Mater. 169 (2009) 70–76.

[14] S. Zodi, O. Potier, F. Lapicque, J.P. Leclerc, Treatment of the industrial wastewaters by electrocoagulation: Optimization of coupled electrochemical and sedimentation processes, Desalination 261 (2010) 186–190.

[15] B. Merzouk, K. Madani, A. Sekki, Treatment characteristics of textile wastewater and removal of heavy metals using the electroflotation technique, Desalination 228 (2008) 245–254.

[16] A.K. Golder, A.N. Samanta, S. Ray, Removal of Cr^{3+} by electrocoagulation with multiple electrodes: Bipolar and monopolar configurations, J. Hazard. Mater. 141 (2007) 653–661.

[17] I. Heidman, W. Calmano, Removal of Cr(VI) from model wastewaters by electrocoagulation with Fe electrode, Sep. Purif. Technol. 61 (2007) 15–21.

[18] X. Chen, G. Chen, P.L. Yue, Separation of pollutants from restaurant wastewater by electrocoagulation, Sep. Purif. Technol. 19 (2000) 65–76.

[19] H. Inan, A. Dimoglo, H. Şimşek, M. Karpuzcu, Olive oil mill wastewater treatment by means of electrocoagulation, Sep. Purif. Technol. 36 (2004) 23–31.

[20] H.A. Moreno-Casillas, D.L. Cocke, J.A.G. Gomes, P. Morkovsky, J.R. Parga, E. Peterson, Electrocoagulation mechanism for COD removal, Sep. Purif. Technol. 56 (2007) 204–211.

[21] M. Khemis, J.P. Leclerc, G. Tanguy, G. Valentin, F. Lapicque, Treatment of industrial liquid wastes by electrocoagulation: Experimental investigations and an overall interpretation model, Chem. Eng. Sci. 61 (2006) 3602–3609.

[22] J.A.G. Gomes, P. Daida, M. Kesmez, M. Weir, H. Moreno, J.R. Parga, G. Irwin, H. McWhinney, T. Grady, E. Peterson, D.L. Cocke, Arsenic removal by electrocoagulation using combined Al–Fe electrode systemand characterization of products, J. Hazard. Mater. 139 (2007) 220–231.

[23] Ş. İrdemez, N. Demircioğlu, Y.S. Yıldız, Z. Bingül, The effects of current density and phosphate concentration on phosphate removal from wastewater by electrocoagulation using aluminum and iron plate electrodes, Sep. Purif. Technol. 52 (2006) 218–223.

[24] N. Mameri, A.R. Yeddou, H. Lounici, D. Belhocine, H. Grib, B. Bariou, Defluoridation of septentrional Sahara water of north Africa by electrocoagulation process using bipolar aluminium electrodes, Water Res. 32 (1998) 1604–1612.

[25] N. Daneshvar, H. Ashassi-Sorkhabi, A. Tizpar, Decolorization of orange II by electrocoagulation method, Sep. Purif. Technol. 31 (2003) 153–162.

[26] X. Chen, G. Chen, P.L. Yue, Investigation on the electrolysis voltage of electrocoagulation, Chem. Eng. Sci. 57 (2002) 2449–2455.

[27] L. Ben Mansour, I. Ksentini, B. Elleuch, Treatment of wastewaters of paper industry by coagulation–electroflotation, Desalination 208 (2007) 34–41.

[28] M.M. Emamjomeh, M. Sivakumar, Review of pollutants removed by electrocoagulation and electrocoagulation/flotation processes, J. Environ. Manage. 90 (2009) 1663–1679.

[29] C.Y. Hu, S.L. Lo, W.H. Kuan, Effects of co-existing anions on fluoride removal in electrocoagulation (EC) process using aluminum electrodes, Water Res. 37 (2003) 4513–4523.

[30] I. Zongo, J.P. Leclerc, H.A. Maïga, J. Wéthé, F. Lapicque, Removal of hexavalent chromium from industrial wastewater by electrocoagulation: A comprehensive comparison of aluminium and iron electrodes, Sep. Purif. Technol. 66 (2009) 159–166.

[31] M. Bayramoglu, M. Eyvaz, M. Kobya, Treatment of the textile wastewater by electrocoagulation, Chem. Eng. J. 128 (2007) 155–161.

[32] O.T. Can, M. Kobya, E. Demirbas, M. Bayramoglu, Treatment of the textile wastewater by combined electrocoagulation, Chemosphere 62 (2006) 181–187.

[33] M. Kobya, E. Demirbas, O.T. Can, M. Bayramoglu, Treatment of levafix orange textile dye solution by electrocoagulation, J. Hazard. Mater. 132 (2006) 183–188.

[34] C.Y. Hu, S.L. Lo, W.H. Kuan, Y.D. Lee, Treatment of high fluoride-content wastewater by continuous electrocoagulation-flotation system with bipolar aluminum electrodes, Sep. Purif. Technol. 60 (2007) 1–5.

[35] N. Daneshvar, A. Oladegaragoze, N. Djafarzadeh, Decolorization of basic dye solutions by electrocoagulation: An investigation of the effect of operational parameters, J. Hazard. Mater. 129 (2006) 116–122.

[36] B. Merzouk, B. Gourich, A. Sekki, K. Madani, Ch. Vial, M. Barkaoui, Studies on the decolorization of textile dye wastewater by continuous electrocoagulation process, Chem. Eng. J. 149 (2009) 207–214.

[37] A.H. Essadki, M. Bennajah, B. Gourich, Ch Vial, M. Azzi, H. Delmas, Electrocoagulation- electroflotation in an external-loop airlift reactor—Application to the decolorization of textile dye wastewater: A case study, Chem. Eng. Process. 47 (2007) 1211–1223.

[38] A. Attour, M. Touati, M. Tlili, M. Ben Amor, F. Lapicque, J.-P. Leclerc, Influence of operating parameters on phosphate removal from water by electrocoagulation using aluminum electrodes, Sep. Purif. Technol. 123 (2014) 124–129.

[39] S. Zodi, B. Merzouk, O. Potier, F. Lapicque, J.-P. Leclerc, Direct red 81 dye removal by a continuous flow electrocoagulation/flotation reactor, Sep. Purif. Technol. 108 (2013) 215–222.